

UC San Diego

UC San Diego Previously Published Works

Title

High affinity CXCR4 inhibitors generated by linking low affinity peptides

Permalink

<https://escholarship.org/uc/item/3n594420>

Authors

Zhang, Chaozai

Huang, Lina S

Zhu, Ruohan

et al.

Publication Date

2019-06-01

DOI

10.1016/j.ejmech.2019.03.056

Peer reviewed



Published in final edited form as:

Eur J Med Chem. 2019 June 15; 172: 174–185. doi:10.1016/j.ejmech.2019.03.056.

High affinity CXCR4 inhibitors generated by linking low affinity peptides

Chaozai Zhang^{a,b}, Lina S. Huang^{a,c}, Ruohan Zhu^d, Qian Meng^d, Siyu Zhu^{a,d}, Yan Xu^d, Huijun Zhang^{a,d}, Xiong Fang^d, Xingquan Zhang^a, Jiao Zhou^e, Robert T. Schooley^a, Xiaohong Yang^{b,*}, Ziwei Huang^{a,*}, Jing An^{a,*}

^aDepartment of Medicine, Division of Infectious Diseases, School of Medicine, University of California San Diego, La Jolla, CA 92037

^bSchool of Pharmaceutical Sciences, Jilin University, Changchun, 130021, China

^cCollege of Arts and Sciences, Cornell University, Ithaca, NY 14853

^dSchool of Life Sciences, Tsinghua University, Beijing, China

^eNobel Institute of Biomedicine, Zhuhai, Guangdong, China

Abstract

G-protein coupled receptors (GPCRs) are implicated in many diseases and attractive targets for drug discovery. Peptide fragments derived from protein ligands of GPCRs are commonly used as probes of GPCR function and as leads for drug development. However, these peptide fragments lack the structural integrity of their parent full-length protein ligands and often show low receptor affinity, which limits their research and therapeutic values. It remains a challenge to efficiently generate high affinity peptide inhibitors of GPCRs. We have investigated a combinational approach involving the synthetic covalent linkage of two low affinity peptide fragments to determine if the strategy can yield high affinity GPCR inhibitors. We examined this design approach using the chemokine receptor CXCR4 as a model GPCR system. Here, we provide a proof of concept demonstration by designing and synthesizing two peptides, AR5 and AR6, that combine a peptide fragment derived from two viral ligands of CXCR4, vMIP-II and HIV-1 envelope glycoprotein gp120. AR5 and AR6 display nanomolar binding affinity, in contrast to the weak micromolar CXCR4 binding of each peptide fragment alone, and inhibit HIV-1 entry via CXCR4. Further studies were carried out for the representative peptide AR6 using western blotting and site-directed mutagenesis in conjunction with molecular dynamic simulation and

*To whom correspondence should be addressed: Jing An: Department of Medicine, Division of Infectious Diseases, School of Medicine, University of California San Diego, La Jolla, CA 92037; jan@ucsd.edu; Ziwei Huang: Department of Medicine, Division of Infectious Diseases, School of Medicine, University of California San Diego, La Jolla, CA 92037; zhuang@ucsd.edu; Xiaohong Yang: School of Pharmaceutical Sciences, Jilin University, Changchun, 130021, China; xiaohongyang88@126.com.

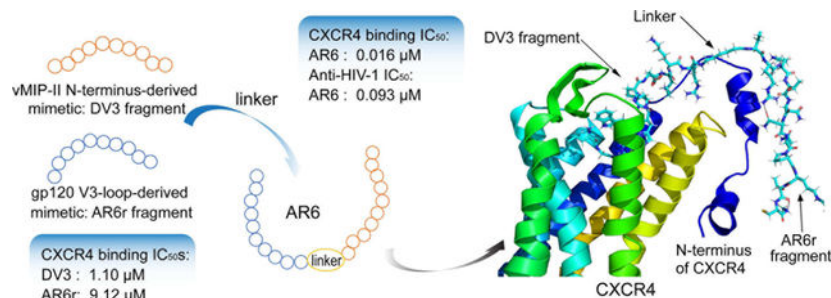
Author Contributions: C.Z., and L.H. designed the peptides, performed the biological experiments, and wrote the manuscript. R.Z. synthesized some of the peptides. Q.M. performed the mapping assays. S.Z. and J. Z. performed the molecular dynamics simulation and binding free energy calculation. Y.X., H.Z., X.Z., and R.T.S. participated in the design of the biological assays and discussion of the data. J.A., Z.H. and X.Y. supervised the work and revised the manuscript.

Publisher's Disclaimer: This is a PDF file of an unedited manuscript that has been accepted for publication. As a service to our customers we are providing this early version of the manuscript. The manuscript will undergo copyediting, typesetting, and review of the resulting proof before it is published in its final citable form. Please note that during the production process errors may be discovered which could affect the content, and all legal disclaimers that apply to the journal pertain.

Conflict of interest: The authors declare that they have no conflicts of interest with the contents of this article.

binding free energy calculation to determine how the peptide interacts with CXCR4 and inhibits its downstream signaling. These results demonstrate that this combinational approach is effective for generating nanomolar active inhibitors of CXCR4 and may be applicable to other GPCRs.

Graphical Abstract



Keywords

drug design; GPCR; chemokine receptor; CXCR4; HIV-1; peptide inhibitors

Introduction

GPCRs are a large family of seven-transmembrane helical proteins that transduce extracellular signals into intracellular responses and are important for a wide variety of biological functions [1, 2]. As the largest class of current therapeutic targets, GPCRs are implicated in many pathological functions and human diseases [3]. Understanding the functions and mechanisms of GPCRs and intervening in the diseases that they mediate require high affinity ligands of GPCRs as tools to dissect their structure-function relationship and leads to develop new drugs [4]. Thus, the development of new methods for discovering high affinity GPCR ligands has been an important goal in chemical biology and translational research of these receptors. In medicinal chemistry, one of the commonly used approaches for generating small molecular ligands of high affinities is to link synthetically two or more moieties or fragments binding different and yet proximal sites of the receptor [5]. For example, two weakly binding small molecules of micromolar affinities were linked to form a nanomolar high affinity ligand [6].

Our laboratories have a long-standing interest in discovering peptide-based ligands of GPCRs [7, 8]. Many GPCRs are known to be recognized by more than one natural ligand. Synthetic peptides derived from certain fragments of a natural ligand involved in the receptor binding have been shown to mimic such binding epitopes of the full-length ligand [9]. However, such peptides often fail to match the affinity of the natural ligand possibly due to the loss of structural stability with particularly short linear peptides and inability to cover all the binding epitopes of the natural ligand. Inspired by the success of the fragment-based approach for small molecules [10], we asked the question whether two weakly binding peptides derived from different natural ligands of the same receptor can be linked to generate a higher affinity ligand in a similar concept used in the medicinal chemistry of small molecular ligands. To test our hypothesis, we used the C-X-C chemokine receptor type 4

(CXCR4, also known as CD184 [11]), a member of the GPCR superfamily as the model system to see whether we can design high affinity ligands based on weakly binding peptide fragments from its natural ligands [7, 8, 12–14]. The chemokine ligands for CXCR4 include its natural, physiological ligand, stromal-derived factor-1 α (SDF-1 α) [15, 16], and a viral chemokine, viral macrophage inflammatory protein-II (vMIP-II) encoded by the herpes virus [17]. CXCR4 is also reported to interact with other proteins such as ubiquitin [18–20]. The interaction of CXCR4 and its natural ligands are involved in many human diseases, including cancer, inflammation and auto-immune diseases [21–29]. The most notable viral ligand of CXCR4 is the envelope glycoprotein gp120 of human immunodeficiency virus type 1 (HIV-1). CXCR4, together with CCR5, are the two principal co-receptors for cellular entry and infection by HIV [30, 31], the etiologic agent for the acquired immune deficiency syndrome (AIDS) [32]. The viral envelope gp120 plays a critical role in the entry of the virus into CD4⁺ T cells, the depletion of which are responsible for the immunodeficiency state that is characteristic of the disease [33]. Binding of HIV-1's gp120 envelope glycoprotein to the cell surface CD4 molecule determines viral tropism and initiates the membrane fusion process [34, 35]. Binding with CD4 induces conformational changes of both gp120 and the CD4 molecule and exposes the third variable (V3) loop of gp120 which is the principal ligand defining binding specificity for entry coreceptor usage [36, 37]. Blocking V3 loop binding to CXCR4 or CCR5 by using neutralizing anti-V3 loop antibodies can effectively inhibit HIV-1 entry and infection [38, 39].

Previously we reported that a synthetic peptide V1 derived from the N-terminus (1–21 residues) of viral macrophage inflammatory protein-II (vMIP-II) and its all-D-amino acid analog DV1 possessed CXCR4 binding affinity and anti-HIV-1 activity [12, 40]. A bivalent, dimeric analog of DV1 showed higher binding affinity than DV1 monomer [41]. Another bivalent analog of DV1 with DV1 linked to DV3, a shorter fragment of DV1 (residues 1–10 of the N-terminus of DV1) displayed high CXCR4 binding affinity [13]. DV3 was also used in another designed peptide SDV3 (DV3-PEG3-K-(PEG3-CXCL12₁₋₈)), an effective CXCR4 agonist [42].

In the present study, we designed and synthesized two peptides, AR5 and AR6, which combine the sequence fragments from the HIV-1 gp120 V3 loop [43–46] and DV3 described above by the covalent linkage of aminohexanoic acid (Ahx). AR5 and AR6 showed significantly increased binding affinity to CXCR4 (IC₅₀ of 18 and 16 nM, respectively) when compared to the peptide fragment from the HIV-1 gp120 V3 loop and DV3 (IC₅₀ > 1 μ M), and they potently inhibited SDF-1 α -induced and CXCR4-mediated calcium influx, cell migration, and ERK phosphorylation, acting as CXCR4 antagonists. Further mutagenesis/mapping, molecular dynamic (MD) simulation and binding free energy calculation studies indicated that Tyr45, Trp94, Asp97 and Tyr116 are important residues for AR6 binding to CXCR4; indeed, Tyr45 and Asp97 are critical for HIV-1 infection [47]. In primary human blood cell-based HIV-1 infection assay, AR6 significantly blocked HIV-1 infection, demonstrating its value as a potential new anti-HIV therapeutic lead.

Results

AR5 and AR6 strongly and competitively inhibit CXCR4 binding to its high affinity antibodies

To determine the CXCR4 binding affinity of the combinational peptides AR5 and AR6, we performed antibody competitive binding assays using CHO-CXCR4 and Sup-T1 cell lines described in previously publications by us or other groups [40, 48–51]. The CHO-CXCR4 cell line was constructed to stably express CXCR4 on its cell surface, whereas the Sup-T1 cell line expresses native CXCR4. The small molecule drug Plerixafor (also known as AMD3100) and DV3 peptide were used for positive controls and comparison.

Both AR5 and AR6 exhibited very high binding affinity for CXCR4, with IC_{50} values of 18 and 16 nM in the CHO-CXCR4 cells and 23 and 14 nM in the Sup-T1 cells, respectively. In contrast, DV3 showed low CXCR4 binding with IC_{50} value of 1.1 μ M on CHO-CXCR4 cell which is similar to the result published previously [42]. AR5r and AR6r, which are peptide fragments derived from the gp120 V3 loop [46, 52], displayed very low CXCR4 affinity, with IC_{50} values of more than 50 μ M and 9.12 μ M, in both the CHO-CXCR4 and the Sup-T1 cells. AR5 and AR6, which combine the two peptide fragments, were 61- and 69-fold more potent than DV3 fragment and 2800- and 570-fold more potent than the AR5r and AR6r fragments alone in both CHO-CXCR4 and Sup-T1 cells (Table 1, Figure 1).

In addition, the length of peptide usually affects the affinity of ligand, the larger size usually means the higher affinity. Actually, some of our previous work has supported the opinion that the length of two linked fragments may affect the affinity of ligands [53, 54]. However, it is not always the case that the larger size peptides will have higher affinity, as optimal lengths are required to produce better binding affinities. For example, (DV3-PEG3)2K has a better binding affinity than (DV3-PEG3) 2K or (DV3-PEG3) 2K [42], whereas AR3 (H2N-Igaswhrpdckclgyqkrplp-Ahx-Kkrffdgll-CONH2) and AR4 (H2N-Igaswhrpdckclgyqkrplp-Ahx- KGLLGLSK-CONH2) are both larger than AR5 or AR6 but they show lower binding affinities (AR3: IC_{50} =193 nM; AR4: IC_{50} =147 nM) when tested under the same conditions (our unpublished data).

AR5 and AR6 block chemotaxis and calcium influx induced by CXCR4's natural ligand SDF-1 α

The functional properties of AR5 and AR6 were evaluated on Sup-T1 cells using CXCR4 chemotaxis and calcium influx assays. AR5 and AR6 both potently blocked the cell migration induced by 50 nM of SDF-1 α (Fig. 2, A and B), with IC_{50} values of 4.03 and 2.87 μ M, respectively. The higher IC_{50} values observed for the chemotaxis assays than for the binding assays may be caused by the following: (1) chemotaxis is much more complicated than receptor binding; more downstream signaling factors could be participating, thereby influencing the final outcome of chemotaxis, and/or (2) the IC_{50} depends on the CXCR4 expression levels in Sup-T1 and CHO-CXCR4 cells. The lower sensitivity of the anti-chemotaxis assay compared to the binding assay may also contribute to the differential inhibitory effects of AR6 on CXCR4 binding versus chemotaxis. In fact,

the different IC₅₀ values for chemotaxis versus CXCR4 binding have been commonly observed in many of our previous studies of CXCR4 inhibitors.

In addition, AR5 and AR6 significantly inhibited the calcium influx induced by 20 nM of SDF-1 α (Fig. 2, C and D). The inhibition was dose dependent. A maximal complete inhibition was achieved in the presence of AR5 or AR6 at 1 μ M. These results show that AR5 and AR6 are antagonists of CXCR4 function.

AR5 and AR6 do not cause CXCR4 internalization

We performed an internalization assay using the CHO-CXCR4 cell line (expressing CXCR4 tagged with a flag at its N-terminus) and FITC-labeled anti-flag antibodies. Various concentrations of SDF-1 α were used as positive controls (Fig. 2E). Following a 1-hour treatment with various concentrations of AR5 and AR6, no CXCR4 internalization was detected in any of the groups. However, SDF-1 α caused a 43.87% CXCR4 internalization after 1h of treatment at 100 nM, which is in agreement with our previous report [55]. This suggested that the inhibitory effect of AR5 and AR6 on competitive 12G5 antibody binding with CXCR4 was not a result of CXCR4 disappearance from the cell surface caused by its cellular internalization.

AR6 inhibits SDF-1 α -induced ERK signaling

SDF-1 α /CXCR4 interactions can trigger AKT and ERK phosphorylation, which accounts for the activated signaling conferred by SDF-1 α . We therefore performed western blot analysis of pERK (phosphor-ERK, pERK) and pAKT (phosphor-AKT, pAKT) in CHO-CXCR4 cells following treatment with SDF-1 α , alone or in combination with AR6 (Fig. 3A). Inclusion of AR6 resulted in downregulation of the basal phosphor-AKT level and strongly abrogated the robust phosphorylation of AKT in cells cotreated with SDF-1 α . Similarly, AR6 downregulated the SDF-1 α induced phospho-AKT levels and also decreased the SDF-1 α -induced phospho-ERK expression. These results indicated that SDF-1 α signaling through CXCR4 activates AKT and ERK and that AR6 inhibits these responses.

AR6 displays potent anti-HIV-1 activity

We performed anti-HIV-1 infection assay on the most potent combinational peptide AR6 by measuring intercellular and extracellular p24 antigen (Fig. 4, A and B). In this assay, PBMCs were infected by NL4-3 virus (X4 strain) [56]. In the one day assay, we found that the presence of AR6 could drastically decrease intracellular p24 after the cells were exposed to the HIV-1 virus. AR6 can decrease the intracellular p24 antigen in AR6 treated groups and is even more effective than AMD3100 at 100 nM. This result demonstrated that AR6 acted as X4 strain HIV-1 entry inhibitors. In a five-day assay, AR6 showed dose-dependent HIV-1 inhibition with the IC₅₀ value of 93 nM (Fig. 4B). Cytotoxicity assays of AR6 were performed in parallel in cells under the same X4 infection and treatment conditions used for anti-HIV-1 assays. In the CellTiter Blue-Based cytotoxicity assays, AR6 showed no cytotoxicity effect with PBMCs when testing cell viability even at the highest concentration of 50 μ M (Fig. 4C). These results demonstrated that AR6 is a potent HIV-1 entry inhibitor and that its anti-HIV-1 activity was not caused by cytotoxic effects on the host cells.

AR6 does not fully overlap with DV3 on CXCR4 binding sites

We conducted ligand binding site-mapping studies using a panel of site-directed CXCR4 mutants to further explore the molecular mechanism of the binding and inhibition of CXCR4 by AR6 (Fig. 5). The mutation sites, which were chosen based on our previous publications, are all located in the transmembrane domains of CXCR4 and critical for the interaction of CXCR4 and vMIP-II or its N-terminal fragment DV1 from which DV3 was derived [41, 47].

Our mutational studies demonstrated that Y45A, W94A, and Y116A decreased AR6 binding affinity, whereas V112A, W195A, Q200A, D262N, and E288Q either did not affect the binding affinity of AR6 or did so less effectively than Y45A, W94A, and Y116A (Fig. 5A). Binding assays using DV3 (the fragment of AR6) alone showed that Y45A, W94A, D97A, Y116A, W195A, D262N, and E288Q could also decrease the binding affinity of DV3, indicating that AR6 and DV3 both interact with Tyr45, Trp94, and Tyr116. The binding results for D97A, V112A, Y116, W195A and D262N revealed differences between AR6 and DV3 with respect to their binding with residues of CXCR4. W195A and D262N decreased the binding affinity of DV3 (Fig. 5B), demonstrating that DV3 could interact with Trp195 and Asp262, whereas AR6 did not show this reduction in binding affinity. Tyr45 is a critical residue for HIV-1 gp120 binding to its co-receptor CXCR4 [14, 41, 57]. Our mapping studies provided further evidence that AR6 could interact with Tyr45 and prevent HIV-1 infection by inhibiting its entry into host cells. The TM domain residue, like Asp97, inhibits the binding activity of AR6 by 15%, but the Asp262 mutation had no effect at all on the AR6 binding activity. The finding that Glu288 and Asp97 are important for SDF-1 α binding, and Glu288 is critical for SDF-1 α signaling, which was demonstrated by our previous publication [57], may explain why the binding activity of AR6 was enhanced by the combinational approach, but no similar enhancement was observed for the inhibition of SDF-1 α -mediated signaling.

AR6 showed an inhibition of SDF-1 α -mediate chemotaxis, calcium flux, and the ERK and AKT signaling against wild type CXCR4. According to the crystal structure of CXCR4 and our mutagenesis results, AR6 or its synthetic analogs can bind with the CXCR4 TM pocket, where the SDF-1 α interacts. Mutations of D97A, Y45A, and D262N affected the binding affinity of AR6 with CXCR4 (Figure 5). Among these mutations, Y45A agreed with our previous results, while others were expanded mutations. Some of the latter mutations were closely adjacent to or around the residues that had been shown as mutated in previous publications and had affected the binding affinity of AR6 with CXCR4 similar to that of DV1, dimer DV1, and DV3[8, 41, 47, 58]. The executive effects of mutations on ligand binding are amino acid dependent; therefore, the E228A, but not the E288Q mutation, was able to affect the binding of CXCR4 with AR6. Stimulation with SDF-1 α can induce the phosphorylation of ERK and AKT in wild-type CXCR4 expressing cells, while the pretreatment of these cells with AR6 can reduce the SDF-1 α -induced phosphorylation of AKT and ERK. These results agreed with previous results that the signaling pathways activated by the SDF-1 α /CXCR4 axis interaction are involved in activation of AKT and ERK[59].

AR6 recognizes two distinct sites of CXCR4 as predicted by molecular modeling

We used molecular modeling/docking and MD simulation studies [60] for further investigation of the interaction between CXCR4 and synthetic combinational peptides by examining the possible binding modes of AR6 with CXCR4 receptor. We estimated a stable CXCR4-AR6 complex by performing a 10 ns MD simulation. AR6 and AR5 were able to recognize two distinct sites or regions of CXCR4 (Fig. 6). The DV3 fragment in these two combinational peptides interacted with residues of the CXCR4 transmembrane helical domains, whereas the other fragments of AR6 (i.e., AR6r derived from a conserved sequences, residues 28–35 of HIV-1 gp120 V3 loop) interacted with the N-terminus of CXCR4, in agreement with results from previous computational studies of the interactions of HIV gp120 V3 loop with CXCR4 reported by others [44].

We calculated the binding free energy between AR6 and CXCR4 using a PDL/S-LRA/ β [61] approach based on the stable MD simulation of the AR6-CXCR4 complex (Table 2), because MD simulation and binding free energy calculation can provide predictable information about the ligand-receptor complex. Wild type (WT), Y45A, W94A, D97A, Y116A, D262N, and E288Q contributed differently to ligand binding, with binding energy contributions of each residue of -11.88 , -7.73 , -10.38 , -13.64 , -6.34 , -11.44 , and -12.67 kcal/mol, respectively (Fig. 6, Table 2). The binding free energy values for the calculated critical residues, such as Tyr45, Trp94, and Tyr116, agreed with the mutational mapping experimental results, indicating that mutations of these residues can lead to a significant binding affinity decrease of CXCR4 and AR6.

Beside the *in silico* simulation, the co-crystal structure of CXCR4 and vMIP-II has provided important evidence that residues in the vMIP-II N terminus and N loop (1-LGASCHRPDKCCLGYQ-16) interact with the CXCR4 TM pocket, CRS1, CRS1.5, and CRS2[62]. The CRS1.5 interaction involves binding of the CXCR4 N-terminal residues 27-PCFR-31 to the vMIP-II residues 8-PDKCC-12. In CRS2, the chemokine N-terminus forms by hydrogen bonds with CXCR4 residues D262, and E288. In addition to this manuscript (and our will soon be published data), our previously publishes data are consistent with the evidence of thee co-crystal structure, according to the following observations: the deletion of the N terminal residues of CXCR4 reduced the activity of HIV-1 entry/infection by 60 to 100% [47], indicating that the N terminal residues of CXCR4 are critical for the interaction of CXCR4 and gp120. For example, the mutation of E288A resulted in a significant reduction in the CXCR4 binding affinity and anti-HIV entry of DV1 and dimer DV1[55]. DV1 is a mimetic of the N-terminal 21 amino acids of vMIP-II, and a partial sequence of the AR6 peptide described in this manuscript. Additional similar results from other groups also showed that the deletion of 32 of the 39 residues of the N-terminal domain of CXCR4 caused resistance in some X4 strains [63]; Mutations of residues in the N terminus (E14/E15, D20, Y21, and D22) reduced the binding of CXCR4 and gp120 [64].

The biological results described above are consistent with the observations made in the molecular modeling study, namely that these fragments, on their own, do recognize CXCR4 but at very low micromolar affinities. This is because each fragment can only interact with one receptor site. Therefore, when combined, they display significantly enhanced nanomolar-level affinities because the simultaneous interactions with two distinctive

receptor sites can lead to much stronger binding. This has commonly been reported for other small molecules using the fragment-based approach of medicinal chemistry.

Discussion

AR5 and AR6 are designed using a fragment based combinational approach that links two low binding affinity fragments derived from viral protein ligands of CXCR4, namely HIV-1 gp120 and viral chemokine vMIP-II [7, 42]. HIV-1, a highly mutated virus, is highly drug resistant. The V3 loop of gp120 is more relatively conserved when compared with the other regions of gp120 [65]. Previously publications reported that 3 sequences of the V3 loop (CTRPNNNTRKSIHIGPGRAFYATGDIIGDIRQAHC) of gp120 are conserved, according to patients' samples or PDB sequence files [46, 66, 67]. Among these 3 conserved sequences, mutation in the V3 stem (residues 3–8 and 26–33) made X4-tropic Envs more sensitive to AMD3100; however, when mutations occurred within the V3 crown (residues 13–20), the Envs retained infectious ability [68]. This information provides the basis for stating that residues of V3 stem are more suitable for peptide design, as simulation of V3 loop binding with CXCR4 and blocks HIV-1 entry. Our newly designed peptide mimics two viral motif sequences (the N- terminus of vMIP-II and the conserved sequences of V3 loop of gp120) and target both the host CXCR4 and the viral HIV-1 conserved regions that are critical for HIV-1 entry and infection. Our data show that AR5 and AR6 interact strongly with CXCR4 with the binding affinities increased from micromoles of the fragments to nanomoles of the combined peptides. The functional characterization of AR5 and AR6 indicates that these combinational peptides can inhibit calcium flux and cell migration induced by SDF-1 α . This suggests that AR5 and AR6 can block downstream signal transduction and that these agents act as CXCR4 antagonists. The mechanistic study of the CXCR4 downstream signals that are induced by SDF-1 α , like pERK and pAKT, indicated that their signals were reduced by AR6. In addition, the mutagenesis mapping data indicated the critical residues for AR6 binding to CXCR4 and some of them are also very important for HIV-1 infection. Furthermore, AR6 shows potent anti-HIV activity with an IC₅₀ value of 93 nM in the five-day p24 assay. AR5 and AR6 both show anti-HIV-1 entry inhibitions at 100 nM in a 24-hour assay and intracellular p24 was decreased. AR5 and AR6 have similar binding affinities to CXCR4; however, the anti-HIV-1 activity was better for AR6 than for AR5 (16 \pm 6.8%, data not shown in this paper). The results of the peptide stability assays may explain these differential anti-HIV-1 effects, as AR6 is more stable than AR5 in serum-containing medium. After the peptides were mixed with medium containing 10% FBS and incubated at 37 °C, AR5 was degraded rapidly, as the peptide HPLC peak at 1 h was only 48% of the original peak, whereas the peptide peak for AR6 was about 80% (data shown in the supplemental materials). In contrast, the unlinked control fragments, DV3 and AR6r alone did not show any antiviral activity. As HIV-1 infection is one of major global health issues, intensive efforts have been undertaken to find effective therapies, resulting in a number of organic compound inhibitors of HIV-1 coreceptors CXCR4 and CCR5 such as AMD3100 and Maraviroc [69, 70]. However, the rapidly emerging drug resistances to current therapies demands more anti- HIV-1 agents of diverse structures and further mechanistic understanding of the molecular interactions underling viral entry and infection. Synthetic peptides provide a class of molecules, different from organic compounds, as

model systems and research tools to study and dissect complex protein-protein interactions involved in viral entry. As shown here, the development of combinational peptides as high affinity ligands mimicking the interactions of different natural viral ligands with the receptor can yield valuable information about the mechanism of protein-protein interactions involving the chemokine receptor family. Taken together, these binding, cellular functional and antiviral results demonstrate the efficacy of the combinational approach in converting low affinity, inactive fragment peptides into high affinity and biologically active agents.

Our findings demonstrate the feasibility of using a peptide fragment-based, combinational approach to generate new high affinity, nanomolar active ligands of CXCR4 receptor with biological activity and potential clinical value. Here, we show that the combination of two weak binding antagonist fragments led to a very strong binding antagonist with potent anti-HIV activity. In another study, we combined a very weak binding agonist fragment with another antagonist fragment and obtained a highly potent combinational peptide which displayed agonistic activities in triggering CXCR4-mediated migration of transplanted neural stem cells in vitro and in a mouse model for regenerative treatment of Sandhoff disease (unpublished data). Thus, our approach as reported here is effective in developing both antagonists and agonists to intervene with different physiological and pathological functions of a GPCR, CXCR4.

Like CXCR4, many GPCRs are known to interact with two or more endogenous or exogenous protein ligands. Often peptide fragments derived from such protein ligands can retain some, although usually quite low, affinity of the native ligand to its receptor. This renders such protein fragment-based peptides less valuable as research tools or therapeutic leads. If the combinational peptide approach, which links two such weakly active fragment peptides to deliver a much stronger ligand as shown here for CXCR4, can be found to be effective for other GPCRs, this approach may become a general and efficient method for the development of high affinity GPCR ligands useful for dissecting GPCR biological functions and treating GPCR-mediated human diseases.

Experimental procedures

Peptides synthesis

The two fragment-based designed peptides, AR5 and AR6 were synthesized by ChinaPeptides Co., Ltd. Both AR5r and AR6r were synthesized automatically with CS Bio Co. Peptide Synthesizer Division by using Fmoc [N-(9-fluorenyl) methoxycarbonyl] chemistry. Fmoc-Rink Amide AM Resin (loading, 0.272 mmol/g, GL) was the solid support. O-(6-Chloro-1-hydrocibenzotriazol-1-yl)-1,1,3,3-tetramethyluronium hexafluorophosphat (HCTU) in N,N-dimethylformamide (DMF) was used as coupling reagent in the presence of diisopropylethylamine (DIEA). 20% (v/v) piperidine in DMF was used to remove Fmoc protection before each coupling reaction. Finished all coupling steps, peptides cleavage and side chain protection removal were treated by mixture of trifluoroacetic acid (TFA), phenol, H₂O and Triisopropylsilane (TIS) (88:2:5:5, v/w/v/v, 10ml) at room temperature for 2 hours. Then TFA was removed by evaporation and peptides were precipitated with ice-cold tert-butylmethyl ether, repeat it twice. Crude peptides were dissolved in mixture of CH₃CN and water and lyophilized. The purity of crude peptide was analyzed by analytical reverse phase

high-performance liquid chromatography (RP-HPLC) and the main peak was collected to characterize by matrix-assisted laser desorption ionization time-of-flight (MALDI-TOF) mass spectrometry. The crude peptides were dissolved in 1:9 CH₃CN/H₂O and purified using semi-preparative RP-HPLC. The solvents we used in HPLC were: A, water with 0.25% TFA; B, CH₃CN with 0.25% TFA in a linear 10% to 40% gradient over 20 minutes with a flow rate of 5 mL/minute. Fraction containing target product were collected together and lyophilized. The peptide powder was stocked at -20 °C for bioassay.

Peripheral blood mononuclear cell (PBMC) isolation

Blood samples were obtained from different healthy donors for each anti-HIV-1 assay, respectively, and diluted with an equal amount of 1× PBS. Approximately 15 mL room temperature Ficoll to a sterile 50 mL tube and then overlaid the Ficoll with 15 mL of diluted blood. After Centrifugation at 1800 rpm for 30 minutes at room temperature, the PBMCs were collected and washed twice with 40 mL 1× PBS by centrifugation (1100 rpm, 10 minutes for each time) at room temperature. Supernatant fluid was discarded and the cell pellet was resuspended in 50 mL RPMI 1640 supplement with 10% FBS and activated with 100 µg/mL PHA (Sigma-Aldrich, USA) for 24 hours. After activation, PBMCs were cultured with RPMI 1640 medium with 10% FBS and 5 IU/mL human Interleukin-2 (hIL-2, Roche Diagnostics, USA) at 37°C with 5% CO₂.

Competitive CXCR4 binding assay

CHO-CXCR4 cells were cultured in RPMI1640 medium with 10% (v/v) FBS, 100 IU penicillin, 0.1 mg/mL streptomycin and 2 mM L-glutamine, and 400 µg/mL geneticin (to maintain stable selection of the CXCR4⁺ CHO cells). After collecting and washing twice with FACS buffer (0.5% BSA, 0.05% sodium azide in PBS) by centrifugation, the CHO cells were then seeded in 96-well v-bottom plates at 5×10⁵ cells/well, and co-incubated with various concentrations of test compounds and primary antibody (1:2000, mouse anti-human CD184 antibody (12G5), BD Biosciences, USA) for 40 minutes on ice. After incubation, cells were washed twice with FACS buffer by centrifugation, and then co-incubated with secondary antibody (1:1000, anti-mouse IgG-FITC antibody, Sigma, USA) for 30 minutes on ice. After two final washings with FACS buffer by centrifugation, FACS buffer was added at 50 µL per well finally. The fluorescence (485_{EX}/528_{EM}) was recorded using a Synergy II plate reader. Experimental data were generated in duplicate each time and from at least three independent experiments. The mean values of fluorescence were normalized and expressed as a percentage of the control group values. Binding curves and IC₅₀ values were calculated by GraphPad Prism 7 and presented as mean ± SEM.

Calcium mobilization assay

SUP-T1 cells were collected and washed twice with assay buffer (HBSS buffer with 20 mM HEPES) by centrifugation. Probenecid (5 µM, Sigma, USA) and Fluo-4AM dye (2 µM, Molecular Probes, USA) were added to cells and incubated in a 37°C cell culture incubator with 5% CO₂ for 30 minutes, with gentle vertexing every 5 minutes. After washing twice with assay buffer, cells at density of 1×10⁶/mL were incubated with various concentrations of test compounds for 2–3 minutes, followed by exposure to 50 nM SDF-1α. The fluorescence (340_{EX}/510_{EM}) was measured using a Synergy II plate reader.

CXCR4 chemotaxis assay

SUP-T1 cells were cultured in RPMI1640 medium containing 10% (v/v) FBS, 100 IU penicillin, 0.1 mg/mL streptomycin and 2 mM L-glutamine. Before performing the chemotaxis assay, SUP-T1 cells were collected and washed twice with assay buffer (RPMI1640 medium with 0.5% BSA) by centrifugation. 1×10^6 cells/well were co-incubated with various concentrations of test compounds for 2 hours, and then seeded in the upper chambers of HTS transwell 96-well plates with a 5 μ m pore size (Corning, USA). The upper chambers were placed into the lower chambers, which contained 200 μ L assay buffer and 20 nM SDF-1 α as chemoattractant. Background groups were cultured by adding only assay buffer in the lower chambers. The transwell plate is placed in a 37°C tissue culture incubator with 5% CO₂ for 3 hours to allow the cells to migrate. Thereafter, the upper chambers were removed and SUP-T1 cells that had migrated to the lower chambers were quantified using CellTiter-Blue cell viability assay reagent (Promega, USA). The fluorescence (560_{EX}/590_{EM}) was recorded using Synergy II microplate reader.

Internalization Assay

The CHO-CXCR4-FLAG cells were collected and washed twice with assay buffer (RPMI 1640 containing 0.5% BSA) by centrifugation at 4°C. Then CHO-CXCR4-FLAG cells were seeded at 3×10^5 cells/well and treated with various concentrations of compounds (SDF-1 α was positive control) for 45 minutes at 37°C. After washing twice with cold PBS, cells were stained with anti-flag antibody (Sigma-Aldrich, Inc., USA) for 30 minutes at 4°C. After the incubation, wash the cells three times with cold PBS and then co-incubate with FITC-labeled anti-mouse antibody for 30 minutes at 4°C. The fluorescence (485_{EX}/528_{EM}) by Synergy II plate reader after washing cells twice with cold PBS.

Western blot

For the western blot analysis, CHO-CXCR4 cells were cultured in DMEM medium (Corning, US) with 10% FBS (Gibco, US). Cells were collected and seeded in 6-well cell culture plate at the concentration of 10^6 cells/well for 24 hours, then treated with medium without FBS. After the incubation, AR6 at 50 μ M was added and co-cultured with cells for 30 minutes, after that SDF-1 α (12.5 nM, PeproTech) was added into each well, incubation for 5 minutes. Subsequently, cells were lysed in PIPA lysis buffer (Beyotime) with Phosphatase Inhibitor Cocktail I (MCE) and the supernatant was collected by centrifugation (12000 rpm, 20 minutes). Lysis buffer was supplemented with a protease inhibitor cocktail (MedChemExpress, MCE). The amount of protein present in the cell lysates was controlled by using a using Enhanced BCA Protein Assay Kit (Beyotime), and the lysates were diluted into the same concentration (3mg/mL) using lysis buffer and boiled at 100°C for 3–4 minutes. Protein extracts were separated in SDS-PAGE (12%) and transferred to nitrocellulose membranes (Millipore). Western blot analysis was performed as previously described [71], blocking the membrane for 1 hour at room temperature using blocking buffer (5% BSA). Incubate the membrane with primary antibody (1:1000 dilution, Cell signaling Technology) in blocking buffer overnight at 4°C. After the incubation, wash the membrane three times using wash buffer (TBST), 5 minutes each. Incubate the membrane with the secondary antibody (1:1000, ZSGB-BIO, CN) in blocking buffer at room temperature for 1

hour. Wash the membrane three times using wash buffer, 5 minutes each. The western blot is visualized using an enhanced chemiluminescent (ECL) substrates kit (Immobilon Western Chemiluminescent HRP Substrate, Millipore).

Anti-HIV assay

Anti-HIV-1 entry assay was performed by measuring intracellular p24 antigen. For a one-day culture test, PBMCs (2.5×10^6 cells/mL) were dispensed into 96-well plates at 100 μ L/well, then co-incubated with compounds of various concentrations for 2 hours. After the incubation, PBMCs were washed twice with PBS and then infected with the NL4-3 strain of HIV-1 at an MOI of 0.02 for 2 hours at 37°C with 5% CO₂. After that, the cells were washed twice with PBS by centrifugation (1200 rpm, 20°C, 5 minutes) and re-suspended with 100 μ L complete medium. After a 24-hour incubation, PBMCs were collected by centrifugation and add 100 μ L lysis buffer with 1% protease inhibitor cocktail (Sigma-Aldrich, USA) was added. The intracellular p24 antigen was tested after lysis of PBMCs following the HIV-1 ELISA kit protocol (PerkinElmer Inc. USA).

For the five-day culture test, the antiviral activity was evaluated by measuring the production of p24 antigen in culture supernatant. Briefly PBMCs (2.5×10^6 cells/mL) were seeded at 100 μ L/well into 96-well plates, then co-incubated with various concentrations of test compounds for 2 hours. After two washes with PBS, the PBMCs were then infected with the NL4-3 strain of HIV-1 at an MOI of 0.001 for 2 hours at 37°C with 5% CO₂, followed by washing twice with PBS by centrifugation (1200rpm, 20°C, 5 minutes) and co-incubated with various concentrations of test compounds. Five days after incubation at 37°C, 20 μ L supernatant were harvested and diluted into 200 μ L for p24 assay. IC₅₀ was calculated by GraphPad Prism 7.

PBMCs viability assay

In parallel with the anti-HIV assays described above, the same densities of PBMCs were seeded and treated with the test compounds for the same periods. After a 5-day incubation at 37°C, the cell viability was determined using CellTiter-Blue (Promega Corporation, USA) cell viability assay. The fluorescence (560_{EX}/590_{EM}) was recorded by Synergy II microplate reader.

Stability of peptide in vitro

AR5 and AR6 were dissolved in the cell culture medium (10% FBS) with a concentration of 1 mM. Samples were collected at different time points of incubation at 37°C and subjected to HPLC analysis with the injection of 10 μ L peptide samples (Microsorb-MV C18 5- μ m, UV 220 nm). The stability of the peptides was calculated based on the changes in the intensity of UV absorbance of the peptides.

Mapping assay using 12G5 antibody

The mapping assays were performed by testing wild type CXCR4 and 10 CXCR4 mutants in competitive binding assays. The binding assay was carried out according to our previous publication [41]. Briefly, a single concentration of AR6 (200 nM) in a final volume of 100 μ L FACS buffer was co-incubated with cells (5×10^5 cells/well) in 96-well plates in the

presence of mouse anti-human CD184 antibody (12G5). Cells were incubated on ice for 30 minutes and washed twice with FACS. Subsequently, the cells were co-incubated with secondary antibody (1:1000, anti-mouse IgG-FITC antibody, Sigma, USA) for 30 minutes on ice. After two final washings with FACS buffer by centrifugation, FACS buffer was added at 50 μ L per well finally. The fluorescence ($485_{EX}/528_{EM}$) was recorded using a Synergy II plate reader. Experimental data were generated in duplicate each time and from at least three independent experiments. The mean values of fluorescence were normalized and expressed as a percentage of the control group values. Binding inhibition column figure was generated using GraphPad Prism 7 and presented as mean \pm SD.

Molecular modeling

The N-terminal residues (1–23) of CXCR4 are important for its recognition by HIV-1 gp120 V3 loop during viral infection of host cells [72]. Since the initial CXCR4 crystal structure template (PDB:4RWS) [62] has the N-terminal (1–22) residues missing, we combined another fragment (PDB:2K05) [73] which contains the missing N-terminal residues (1–22) of 4RWS by using the I-TASSER server (an online server which is used for protein structure prediction) to model the missing N-terminal residues (Job number: S350286) [74]. The 2K05 is an NMR structure. We chose this structure mainly because of its N-terminal sequence of CXCR4, which allowed us to generate a complete CXCR4 structure with the N-terminus for molecular docking and dynamic simulation. Following the I-TASSER on-line server guidance, a full CXCR4 sequence was put in and CXCR4 in the complex of 4RWS was used as a template for the structure prediction [75]. The peptide structures were constructed by using ChemDraw software and docked with CXCR4 molecule as described in our previous publication [41].

We used the MOLARIS software [76] to conduct MD simulation and calculations of binding free energies. Before performing the binding free energy calculations, the protein-ligand complex was selected from molecular docking. The binding free energy was calculated using semi macroscopic protein dipoles Langevin dipoles-linear response approximation/ β (PDL/S-LRA/ β) which is capable of assessing contributions to the binding free energy from hydrophobic effects, vdW, and water penetration [61]. The MD simulations were performed using the standard MOLARIS surface constrained all-atom solvent (SCAAS) [77] boundary conditions and the local reaction field (LRF) long-range treatment [78]. The simulation system involved an explicit all atoms water sphere of 18 \AA , solvating the protein-ligand complex, where the surface waters are subject to polarization and radial restraint to make the finite system behave as if it is part of an infinite system. This 18 \AA simulation sphere surrounded by a 2 \AA Langevin dipole surface imbedded in a bulk continuum. The PDL/S-LRA/ β calculation involved a replacement of the explicit all-atoms waters by Langevin dipoles. The simulations were performed following the previously reported procedure [79]. Initial relaxation was performed for 90 ps by gradually heating to a target temperature of 300 K using the polarizable ENZYMIK force field. After that the ligand sequence was defined as region I (see Figure 2 of ref. 63) and relaxation dynamics for 90 ps, dynamics in water for 24 ps, and dynamics in the protein for 24 ps with a step size of 1.0 fs were performed respectively to generate five configurations, which were automatically used

to calculate the binding free energy using Eq. 13 of ref. 63 with the POLARIS module of MOLARIS.

Statistical analysis

Statistical analysis was performed using the one-way ANOVA (GraphPad Software: GraphPad Prism 7 for Windows). Average values were expressed as mean \pm SD or SEM, n 3. The results of calcium influxes/effluxes and western blots were representatives of at least of three independent experiments. A P value less than 0.05 was considered statistically significant.

Supplementary Material

Refer to Web version on PubMed Central for supplementary material.

Acknowledgments:

We would like to thank Drs. Dibyendu Mondal and Arieh Warshel (Department of Chemistry, University of Southern California) for providing the computational software used in this study and discussion of the computational results. This work was supported by grants from the National Institutes of Health (GM 57761, to Z.H and J.A.), and the California Institute for Regenerative Medicine (to Z.H.). C.Z. was supported in part by the Chinese Scholarship Council.

Abbreviations

Ahx	aminohexanoic acid
AIDS	acquired immune deficiency syndrome
CXCR4	C-X-C chemokine receptor type 4
DIEA	diisopropylethylamine
DMF	N, N-dimethylformamide
GPCR	G-protein coupled receptor
HCTU	O-(6-Chloro-1-hydrocibenzotriazol-1-yl)-1,1,3,3-tetramethyluronium hexafluorophosphate
HIV-1	human immunodeficiency virus type 1
LRF	local reaction field
MALDI-TOF	matrix-assisted laser desorption ionization time-of-flight
MD	molecular dynamic
pAKT	phosphor-AKT
PBMC	peripheral blood mononuclear cell
PDL/D/S-LRA/β	protein dipoles Langevin dipoles-linear response approximation/ β

pERK	phosphor-ERK
RP-HPLC	analytical reverse phase high-performance liquid chromatography
SCAAS	surface constrained all-atom solvent
SDF-1α	Stromal cell-derived factor 1 alpha
TFA	trifluoroacetic acid
TIS	Triisopropylsilane
vMIP-II	viral macrophage inflammatory protein-II
WT	wild type

References

- [1]. Rosenbaum DM, Rasmussen SG, Kobilka BK, The structure and function of G-protein- coupled receptors, *Nature*, 459 (2009) 356–363. [PubMed: 19458711]
- [2]. Hilger D, Masureel M, Kobilka BK, Structure and dynamics of GPCR signaling complexes, *Nat Struct Mol Biol*, 25 (2018) 4–12. [PubMed: 29323277]
- [3]. Heng BC, Aubel D, Fussenegger M, An overview of the diverse roles of G-protein coupled receptors (GPCRs) in the pathophysiology of various human diseases, *Biotechnol Adv*, 31 (2013) 1676–1694. [PubMed: 23999358]
- [4]. Hauser AS, Attwood MM, Rask-Andersen M, Schiøth HB, Gloriam DE, Trends in GPCR drug discovery: new agents, targets and indications, *Nat Rev Drug Discov*, 16 (2017) 829–842. [PubMed: 29075003]
- [5]. Harner MJ, Frank AO, Fesik SW, Fragment-based drug discovery using NMR spectroscopy, *J Biomol NMR*, 56 (2013) 65–75. [PubMed: 23686385]
- [6]. Shuker SB, Hajduk PJ, Meadows RP, Fesik SW, Discovering high-affinity ligands for proteins: SAR by NMR, *Science*, 274 (1996) 1531–1534. [PubMed: 8929414]
- [7]. Huang Z, Structural chemistry and therapeutic intervention of protein-protein interactions in immune response, human immunodeficiency virus entry, and apoptosis, *Pharmacol Ther*, 86 (2000) 201–215. [PubMed: 10882809]
- [8]. Choi W, Duggineni S, Xu Y, Huang Z, An J, Drug discovery research targeting the CXC chemokine receptor 4 (CXCR4), *Journal of Medicinal Chemistry*, 55 (2012) 977–994. [PubMed: 22085380]
- [9]. Pelay-Gimeno M, Glas A, Koch O, Grossmann TN, Structure-Based Design of Inhibitors of Protein-Protein Interactions: Mimicking Peptide Binding Epitopes, *Angew Chem Int Ed Engl*, 54 (2015) 8896–8927. [PubMed: 26119925]
- [10]. Scott DE, Coyne AG, Hudson SA, Abell C, Fragment-based approaches in drug discovery and chemical biology, *Biochemistry*, 51 (2012) 4990–5003. [PubMed: 22697260]
- [11]. Mason D, Andre P, Bensussan A, Buckley C, Civin C, Clark E, de Haas M, Goyert S, Hadam M, Hart D, Horejsi V, Meuer S, Morrissey J, Schwartz-Albiez R, Shaw S, Simmons D, Ugucioni M, van der Schoot E, Vivier E, Zola H, CD antigens 2002, *Blood*, 99 (2002) 3877–3880. [PubMed: 12014373]
- [12]. Luo Z, Fan X, Zhou N, Hiraoka M, Luo J, Kaji H, Huang Z, Structure-function study and anti-HIV activity of synthetic peptide analogues derived from viral chemokine vMIP-II, *Biochemistry*, 39 (2000) 13545–13550. [PubMed: 11063591]
- [13]. Xu Y, Duggineni S, Espitia S, Richman DD, An J, Huang Z, A synthetic bivalent ligand of CXCR4 inhibits HIV infection, *Biochem Biophys Res Commun*, 435 (2013) 646–650. [PubMed: 23688427]

- [14]. Choi WT, Tian S, Dong CZ, Kumar S, Liu D, Madani N, An J, Sodroski JG, Huang Z, Unique ligand binding sites on CXCR4 probed by a chemical biology approach: implications for the design of selective human immunodeficiency virus type 1 inhibitors, *J Virol*, 79 (2005) 15398–15404. [PubMed: 16306611]
- [15]. Busillo JM, Benovic JL, Regulation of CXCR4 signaling, *Biochim Biophys Acta*, 1768 (2007) 952–963. [PubMed: 17169327]
- [16]. Barbero S, Bonavia R, Bajetto A, Porcile C, Pirani P, Ravetti JL, Zona GL, Spaziante R, Florio T, Schettini G, Stromal Cell-derived Factor 1 α Stimulates Human Glioblastoma Cell Growth through the Activation of Both Extracellular Signal-regulated Kinases 1/2 and Akt, *Cancer Research*, 63 (2003) 1969–1974. [PubMed: 12702590]
- [17]. Moore PS, Boshoff C, Weiss RA, Chang Y, Molecular mimicry of human cytokine and cytokine response pathway genes by KSHV, *Science*, 274 (1996) 1739–1744. [PubMed: 8939871]
- [18]. Saini V, Staren DM, Ziarek JJ, Nashaat ZN, Campbell EM, Volkman BF, Marchese A, Majetschak M, The CXC chemokine receptor 4 ligands ubiquitin and stromal cell-derived factor-1 α function through distinct receptor interactions, *J Biol Chem*, 286 (2011) 33466–33477. [PubMed: 21757744]
- [19]. Saini V, Marchese A, Majetschak M, CXC chemokine receptor 4 is a cell surface receptor for extracellular ubiquitin, *J Biol Chem*, 285 (2010) 15566–15576. [PubMed: 20228059]
- [20]. Saini V, Marchese A, Tang WJ, Majetschak M, Structural determinants of ubiquitin-CXC chemokine receptor 4 interaction, *J Biol Chem*, 286 (2011) 44145–44152. [PubMed: 22039044]
- [21]. Gonzalo JA, Lloyd CM, Peled A, Delaney T, Coyle AJ, Gutierrez-Ramos JC, Critical involvement of the chemotactic axis CXCR4/stromal cell-derived factor-1 α in the inflammatory component of allergic airway disease, *J Immunol*, 165 (2000) 499–508. [PubMed: 10861089]
- [22]. Popik W, Hesselgesser JE, Pitha PM, Binding of human immunodeficiency virus type 1 to CD4 and CXCR4 receptors differentially regulates expression of inflammatory genes and activates the MEK/ERK signaling pathway, *J Virol*, 72 (1998) 6406–6413. [PubMed: 9658081]
- [23]. Gupta SK, Lysko PG, Pillarisetti K, Ohlstein E, Stadel JM, Chemokine receptors in human endothelial cells. Functional expression of CXCR4 and its transcriptional regulation by inflammatory cytokines, *J Biol Chem*, 273 (1998) 4282–4287. [PubMed: 9461627]
- [24]. Hogaboam CM, Carpenter KJ, Schuh JM, Proudfoot AA, Bridger G, Buckland KF, The therapeutic potential in targeting CCR5 and CXCR4 receptors in infectious and allergic pulmonary disease, *Pharmacol Ther*, 107 (2005) 314–328. [PubMed: 16009428]
- [25]. Burger M, Glodek A, Hartmann T, Schmitt-Graff A, Silberstein LE, Fujii N, Kipps TJ, Burger JA, Functional expression of CXCR4 (CD184) on small-cell lung cancer cells mediates migration, integrin activation, and adhesion to stromal cells, *Oncogene*, 22 (2003) 8093–8101. [PubMed: 14603250]
- [26]. Taichman RS, Cooper C, Keller ET, Pienta KJ, Taichman NS, McCauley LK, Use of the stromal cell-derived factor-1/CXCR4 pathway in prostate cancer metastasis to bone, *Cancer Res*, 62 (2002) 1832–1837. [PubMed: 11912162]
- [27]. Wang C, Cheng H, Li Y, Role of SDF-1 and CXCR4 in the proliferation, migration and invasion of cervical cancer, *Pak J Pharm Sci*, 29 (2016) 2151–2154. [PubMed: 28412671]
- [28]. Murphy PM, The molecular biology of leukocyte chemoattractant receptors, *Annu Rev Immunol*, 12 (1994) 593–633. [PubMed: 8011292]
- [29]. Choi WT, An J, Biology and clinical relevance of chemokines and chemokine receptors CXCR4 and CCR5 in human diseases, *Exp Biol Med (Maywood)*, 236 (2011) 637–647. [PubMed: 21565895]
- [30]. Feng Y, Broder CC, Kennedy PE, Berger EA, HIV-1 entry cofactor: functional cDNA cloning of a seven-transmembrane, G protein-coupled receptor, *Science*, 272 (1996) 872–877. [PubMed: 8629022]
- [31]. Alkhatib G, Combadiere C, Broder CC, Feng Y, Kennedy PE, Murphy PM, Berger EA, CC CKR5: a RANTES, MIP-1 α , MIP-1 β receptor as a fusion cofactor for macrophage-tropic HIV-1, *Science*, 272 (1996) 1955–1958. [PubMed: 8658171]

- [32]. Barre-Sinoussi F, Chermann JC, Rey F, Nugeyre MT, Chamaret S, Gruest J, Dautet C, Axler-Blin C, Vezinet-Brun F, Rouzioux C, Rozenbaum W, Montagnier L, Isolation of a T-lymphotropic retrovirus from a patient at risk for acquired immune deficiency syndrome (AIDS), *Science*, 220 (1983) 868–871. [PubMed: 6189183]
- [33]. Klatzmann D, Champagne E, Chamaret S, Gruest J, Guetard D, Hercend T, Gluckman JC, Montagnier L, T-lymphocyte T4 molecule behaves as the receptor for human retrovirus LAV, *Nature*, 312 (1984) 767–768. [PubMed: 6083454]
- [34]. Chan DC, Kim PS, HIV entry and its inhibition, *Cell*, 93 (1998) 681–684. [PubMed: 9630213]
- [35]. Wilen CB, Tilton JC, Doms RW, HIV: cell binding and entry, *Cold Spring Harb Perspect Med*, 2 (2012).
- [36]. Speck RF, Wehrly K, Platt EJ, Atchison RE, Charo IF, Kabat D, Chesebro B, Goldsmith MA, Selective employment of chemokine receptors as human immunodeficiency virus type 1 coreceptors determined by individual amino acids within the envelope V3 loop, *J Virol*, 71 (1997) 7136–7139. [PubMed: 9261451]
- [37]. Cocchi F, DeVico AL, Garzino-Demo A, Cara A, Gallo RC, Lusso P, The V3 domain of the HIV-1 gp120 envelope glycoprotein is critical for chemokine-mediated blockade of infection, *Nat Med*, 2 (1996) 1244–1247. [PubMed: 8898753]
- [38]. Valenzuela A, Blanco J, Krust B, Franco R, Hovanessian AG, Neutralizing antibodies against the V3 loop of human immunodeficiency virus type 1 gp120 block the CD4-dependent and -independent binding of virus to cells, *J Virol*, 71 (1997) 8289–8298. [PubMed: 9343181]
- [39]. Tilley SA, Honnen WJ, Racho ME, Chou TC, Pinter A, Synergistic neutralization of HIV-1 by human monoclonal antibodies against the V3 loop and the CD4-binding site of gp120, *AIDS Res Hum Retroviruses*, 8 (1992) 461–467. [PubMed: 1376135]
- [40]. Zhou N, Luo Z, Luo J, Fan X, Cayabyab M, Hiraoka M, Liu D, Han X, Pesavento J, Dong CZ, Wang Y, An J, Kaji H, Sodroski JG, Huang Z, Exploring the stereochemistry of CXCR4-peptide recognition and inhibiting HIV-1 entry with D-peptides derived from chemokines, *J Biol Chem*, 277 (2002) 17476–17485. [PubMed: 11880384]
- [41]. Choi WT, Kumar S, Madani N, Han X, Tian S, Dong CZ, Liu D, Duggineni S, Yuan J, Sodroski JG, Huang Z, An J, A novel synthetic bivalent ligand to probe chemokine receptor CXCR4 dimerization and inhibit HIV-1 entry, *Biochemistry*, 51 (2012) 7078–7086. [PubMed: 22897429]
- [42]. Yang Y, Gao M, Zhang Q, Zhang C, Yang X, Huang Z, An J, Design, synthesis, and biological characterization of novel PEG-linked dimeric modulators for CXCR4, *Bioorg Med Chem*, 24 (2016) 5393–5399. [PubMed: 27658790]
- [43]. Rawi R, Kunji K, Haoudi A, Bensmail H, Coevolution Analysis of HIV-1 Envelope Glycoprotein Complex, *PLoS One*, 10 (2015) e0143245. [PubMed: 26579711]
- [44]. Tamamis P, Floudas CA, Molecular recognition of CXCR4 by a dual tropic HIV-1 gp120 V3 loop, *Biophys J*, 105 (2013) 1502–1514. [PubMed: 24048002]
- [45]. Bagnarelli P, Fiorelli L, Vecchi M, Monchetti A, Menzo S, Clementi M, Analysis of the functional relationship between V3 loop and gp120 context with regard to human immunodeficiency virus coreceptor usage using naturally selected sequences and different viral backbones, *Virology*, 307 (2003) 328–340. [PubMed: 12667802]
- [46]. Schreiber M, Wachsmuth C, Muller H, Odemuyiwa S, Schmitz H, Meyer S, Meyer B, Schneider-Mergener J, The V3-directed immune response in natural human immunodeficiency virus type 1 infection is predominantly directed against a variable, discontinuous epitope presented by the gp120 V3 domain, *J Virol*, 71 (1997) 9198–9205. [PubMed: 9371578]
- [47]. Choi W, Tian S, Dong C, Kumar S, Liu D, Madani N, An J, Sodroski J, Huang Z, Unique Ligand Binding Sites on CXCR4 Probed by a Chemical Biology Approach: Implications for the Design of Selective Human Immunodeficiency Virus Type 1 Inhibitors, *Journal of Virology*, 79 (2005) 15398–15404. [PubMed: 16306611]
- [48]. Yang Y, Zhang Q, Gao M, Yang X, Huang Z, An J, A novel CXCR4-selective high-affinity fluorescent probe and its application in competitive binding assays, *Biochemistry*, 53 (2014) 4881–4883. [PubMed: 25058910]
- [49]. Wester HJ, Keller U, Schottelius M, Beer A, Philipp-Abbrederis K, Hoffmann F, Simecek J, Gerngross C, Lassmann M, Herrmann K, Pellegata N, Rudelius M, Kessler H, Schwaiger M,

Disclosing the CXCR4 Expression in Lymphoproliferative Diseases by Targeted Molecular Imaging, *Theranostics*, 5 (2015) 618–630. [PubMed: 25825601]

- [50]. Hulme EC, Trevethick MA, Ligand binding assays at equilibrium: validation and interpretation, *Br J Pharmacol*, 161 (2010) 1219–1237. [PubMed: 20132208]
- [51]. Yang J, Copeland RA, Lai Z, Defining balanced conditions for inhibitor screening assays that target bisubstrate enzymes, *J Biomol Screen*, 14 (2009) 111–120. [PubMed: 19196704]
- [52]. Pollakis G, Kang S, Kliphuis A, Chalaby MI, Goudsmit J, Paxton WA, N-linked glycosylation of the HIV type-1 gp120 envelope glycoprotein as a major determinant of CCR5 and CXCR4 coreceptor utilization, *J Biol Chem*, 276 (2001) 13433–13441. [PubMed: 11278567]
- [53]. Kumar S, Choi WT, Dong CZ, Madani N, Tian S, Liu D, Wang Y, Pesavento J, Wang J, Fan X, Yuan J, Fritzsche WR, An J, Sodroski JG, Richman DD, Huang Z, SMM-chemokines: a class of unnatural synthetic molecules as chemical probes of chemokine receptor biology and leads for therapeutic development, *Chem Biol*, 13 (2006) 69–79. [PubMed: 16426973]
- [54]. Zhou N, Luo Z, Luo J, Fan X, Cayabyab MJ, Hiraoka M, Liu D, Han X, Pesavento JJ, Dong C, Exploring the Stereochemistry of CXCR4-Peptide Recognition and Inhibiting HIV-1 Entry with D-Peptides Derived from Chemokines*, *Journal of Biological Chemistry*, 277 (2002) 17476–17485. [PubMed: 11880384]
- [55]. Dong CZ, Tian S, Choi WT, Kumar S, Liu D, Xu Y, Han X, Huang Z, An J, Critical role in CXCR4 signaling and internalization of the polypeptide main chain in the amino terminus of SDF-1 α probed by novel N-methylated synthetically and modularly modified chemokine analogues, *Biochemistry*, 51 (2012) 5951–5957. [PubMed: 22779681]
- [56]. Douek DC, Brenchley JM, Betts MR, Ambrozak DR, Hill BJ, Okamoto Y, Casazza JP, Kuruppu J, Kunstman K, Wolinsky S, Grossman Z, Dybul M, Oxenius A, Price DA, Connors M, Koup RA, HIV preferentially infects HIV-specific CD4⁺ T cells, *Nature*, 417 (2002) 95–98. [PubMed: 11986671]
- [57]. Tian S, Choi WT, Liu D, Pesavento J, Wang Y, An J, Sodroski JG, Huang Z, Distinct functional sites for human immunodeficiency virus type 1 and stromal cell-derived factor 1 α on CXCR4 transmembrane helical domains, *J Virol*, 79 (2005) 12667–12673. [PubMed: 16188969]
- [58]. Tian S, Choi W, Liu D, Pesavento JJ, Wang Y, An J, Sodroski J, Huang Z, Distinct Functional Sites for Human Immunodeficiency Virus Type 1 and Stromal Cell-Derived Factor 1 α on CXCR4 Transmembrane Helical Domains, *Journal of Virology*, 79 (2005) 12667–12673. [PubMed: 16188969]
- [59]. Mao Y, Meng Q, Song P, Zhu S, Xu Y, Snyder EY, An J, Huang Z, Novel Bivalent and D- Peptide Ligands of CXCR4 Mobilize Hematopoietic Progenitor Cells to the Blood in C3H/HeJ Mice, *Cell Transplant*, 27 (2018) 1249–1255. [PubMed: 29991278]
- [60]. Kawatkar SP, Yan M, Gevariya H, Lim MY, Eisold S, Zhu X, Huang Z, An J, Computational analysis of the structural mechanism of inhibition of chemokine receptor CXCR4 by small molecule antagonists, *Exp Biol Med (Maywood)*, 236 (2011) 844–850. [PubMed: 21697335]
- [61]. Singh N, Warshel A, Absolute binding free energy calculations: on the accuracy of computational scoring of protein-ligand interactions, *Proteins*, 78 (2010) 1705–1723. [PubMed: 20186976]
- [62]. Qin L, Kufareva I, Holden LG, Wang C, Zheng Y, Zhao C, Fenalti G, Wu H, Han GW, Cherezov V, Abagyan R, Stevens RC, Handel TM, Structural biology. Crystal structure of the chemokine receptor CXCR4 in complex with a viral chemokine, *Science*, 347 (2015) 1117–1122. [PubMed: 25612609]
- [63]. Labrosse B, Treboute C, Brelot A, Alizon M, Cooperation of the V1/V2 and V3 Domains of Human Immunodeficiency Virus Type 1 gp120 for Interaction with the CXCR4 Receptor, *Journal of Virology*, 75 (2001) 5457. [PubMed: 11356952]
- [64]. Brelot A, Heveker N, Montes M, Alizon M, Identification of residues of CXCR4 critical for human immunodeficiency virus coreceptor and chemokine receptor activities, *J Biol Chem*, 275 (2000) 23736–23744. [PubMed: 10825158]
- [65]. Jiang X, Burke V, Totrov M, Williams C, Cardozo T, Gorny MK, Zolla-Pazner S, Kong X-P, Conserved structural elements in the V3 crown of HIV-1 gp120, *Nature Structural & Molecular Biology*, 17 (2010) 955.

- [66]. Itescu S, Simonelli PF, Winchester RJ, Ginsberg HS, Human immunodeficiency virus type 1 strains in the lungs of infected individuals evolve independently from those in peripheral blood and are highly conserved in the C-terminal region of the envelope V3 loop, *Proc Natl Acad Sci U S A*, 91 (1994) 11378–11382. [PubMed: 7972068]
- [67]. Huang CC, Lam SN, Acharya P, Tang M, Xiang SH, Hussan SSU, Stanfield RL, Robinson J, Sodroski J, Wilson IA, Wyatt R, Bewley CA, Kwong PD, Structures of the CCR5 N terminus and of a tyrosine-sulfated antibody with HIV-1 gp120 and CD4, *Science*, 317 (2007) 1930–1934. [PubMed: 17901336]
- [68]. Nolan KM, Jordan APO, Hoxie JA, Effects of Partial Deletions within the Human Immunodeficiency Virus Type 1 V3 Loop on Coreceptor Tropism and Sensitivity to Entry Inhibitors, *Journal of Virology*, 82 (2008) 664. [PubMed: 17977968]
- [69]. Hendrix CW, Collier AC, Lederman MM, Schols D, Pollard RB, Brown S, Jackson JB, Coombs RW, Glesby MJ, Flexner CW, Bridger GJ, Badel K, MacFarland RT, Henson GW, Calandra G, Group AHS, Safety, pharmacokinetics, and antiviral activity of AMD3100, a selective CXCR4 receptor inhibitor, in HIV-1 infection, *J Acquir Immune Defic Syndr*, 37 (2004) 1253–1262. [PubMed: 15385732]
- [70]. Fatkenheuer G, Nelson M, Lazzarin A, Konourina I, Hoepelman AIM, Lampiris H, Hirschel B, Tebas P, Raffi F, Trottier B, Bellos N, Saag M, Cooper DA, Westby M, Tawadrous M, Sullivan JF, Ridgway C, Dunne MW, Felstead S, Mayer H, van der Ryst E, Team MS, Team MS, Subgroup analyses of Maraviroc in previously treated R5 HIV-1 infection, *New Engl J Med*, 359 (2008) 1442–U1446. [PubMed: 18832245]
- [71]. Zeng Z, Samudio I, Munsell MF, An J, Huang Z, Estey EH, Andreeff M, Konopleva M, Inhibition of CXCR4 with the novel RCP168 peptide overcomes stroma-mediated chemoresistance in chronic and acute leukemias, *Molecular Cancer Therapeutics*, 5 (2006) 3113–3121. [PubMed: 17172414]
- [72]. Islam S, Hoque SA, Adnan N, Tanaka A, Jinno-Oue A, Hoshino H, X4-tropic human immunodeficiency virus IIIB utilizes CXCR4 as coreceptor, as distinct from R5X4-tropic viruses, *Microbiol Immunol*, 57 (2013) 437–444. [PubMed: 23773022]
- [73]. Veldkamp CT, Seibert C, Peterson FC, De la Cruz NB, Haugner JC 3rd, Basnet H, Sakmar TP, Volkman BF, Structural basis of CXCR4 sulfotyrosine recognition by the chemokine SDF-1/CXCL12, *Sci Signal*, 1 (2008) ra4. [PubMed: 18799424]
- [74]. Zhang Y, I-TASSER server for protein 3D structure prediction, *BMC Bioinformatics*, 9 (2008) 40. [PubMed: 18215316]
- [75]. Roy A, Kucukural A, Zhang Y, I-TASSER: a unified platform for automated protein structure and function prediction, *Nat Protoc*, 5 (2010) 725–738. [PubMed: 20360767]
- [76]. Mukherjee S, Alhadeff R, Warshel A, Simulating the dynamics of the mechanochemical cycle of myosin-V, *P Natl Acad Sci USA*, 114 (2017) 2259–2264.
- [77]. King G, Warshel A, A surface constrained all-atom solvent model for effective simulations of polar solutions, *Journal of Chemical Physics*, 91 (1989) 3647–3661.
- [78]. Lee FS, Warshel A, A local reaction field method for fast evaluation of long-range electrostatic interactions in molecular simulations, *Journal of Chemical Physics*, 97 (1992) 3100–3107.
- [79]. Sham YY, Chu ZT, Tao H, Warshel A, Examining methods for calculations of binding free energies: LRA, LIE, PDL-D-LRA, and PDL-D/S-LRA calculations of ligands binding to an HIV protease, *Proteins*, 39 (2000) 393–407. [PubMed: 10813821]

Highlights

- A combinational approach yielding high affinity GPCR inhibitors was demonstrated in the CXCR4 system
- Novel combinational peptides, such as AR6, were identified with nanomolar binding affinities for CXCR4
- AR6 acts as a CXCR4 antagonist and inhibits HIV-1 entry via CXCR4 at a nanomolar level
- How AR6 interacts with CXCR4 and inhibits its downstream signaling was examined

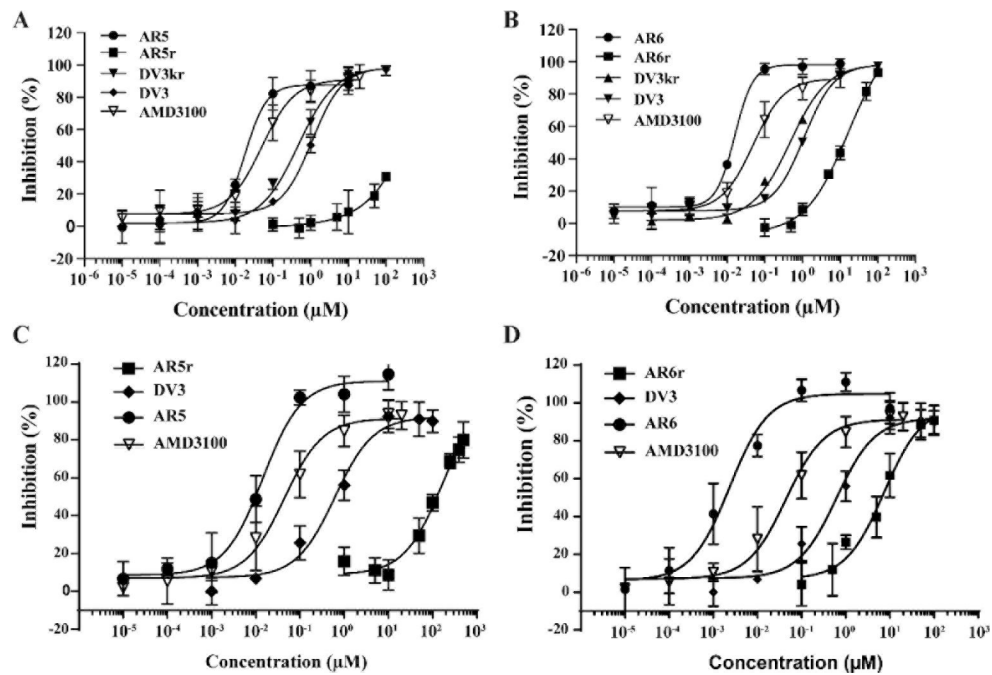


Figure 1.

Competitive binding activities of CXCR4 ligands. The IC_{50} values of the test compounds were determined by 12G5 antibody competition binding assays by using CHO- CXCR4 (A and B) and Sup-T1 cells (C and D). AMD3100 and DV3 were used as positive controls. The results are the mean values of at least three independent experiments.

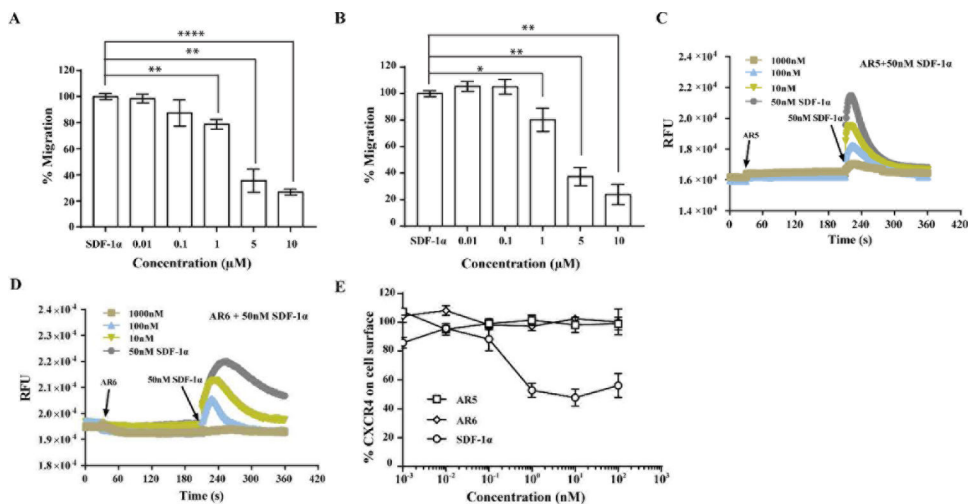


Figure 2.

Functional characterizations of AR5 and AR6. **A, B**) Chemotaxis inhibition activities of AR5 (**A**) and AR6 (**B**). Chemotaxis inhibition was expressed as the percentage of SUP-T1 cells initially seeded in the upper chambers of 5 μM core size transwells that migrated into the bottom chambers following stimulation by 20 nM SDF-1 α . The IC₅₀ values were calculated by GraphPad Prism 7 and the results are mean \pm SD of at least three independent experiments. *, p value < 0.05, **, p value < 0.005, ****, p value < 0.00005. **C, D**) Calcium influx inhibitory activities of AR5 (**C**) and AR6 (**D**) against 50 nM SDF-1 α . AR5 and AR6 at 1 mM almost completely inhibited the calcium influx induced by 50 nM SDF-1 α . **E**) CXCR4 internalization in response to AR5 and AR6. CHO-CXCR4 cells express a tag in the N-terminus of CXCR4 and FITC-labeled anti-FLAG antibody was used to measure CXCR4 internalization after exposure to AR5 and AR6. SDF-1 α was used as a positive control. AR5 and AR6 showed no detectable activities in producing CXCR4 internalization. The results are mean \pm SEM of at least three independent experiments.

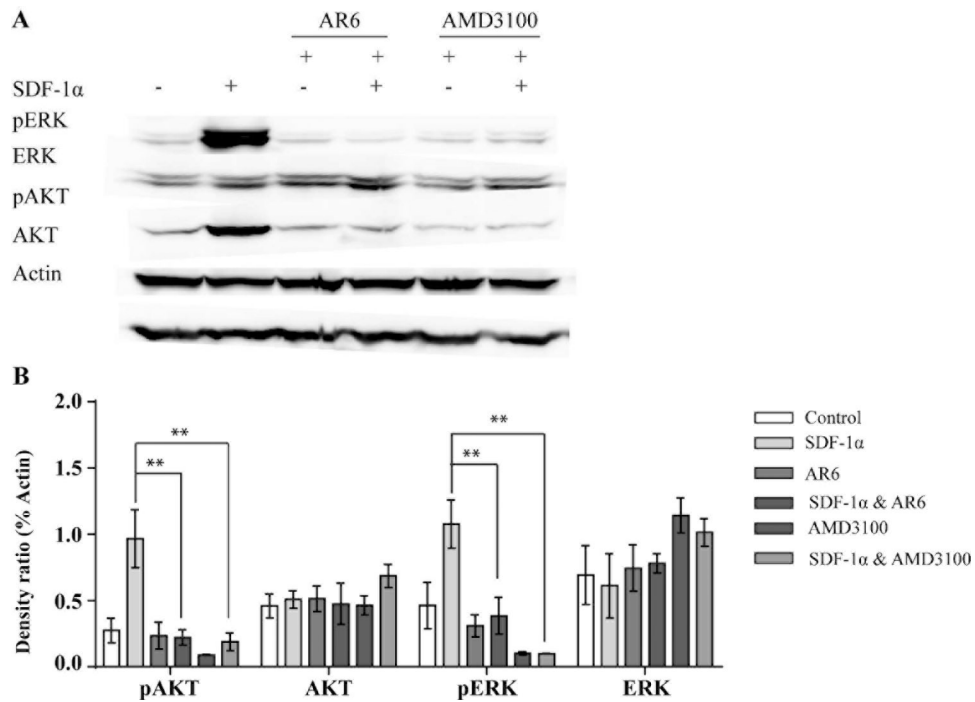


Figure 3. AR6 inhibited SDF-1 α -activated signaling pathways. CHO-CXCR4 cells were left untreated or exposed to 12.5 nM SDF-1 α , alone or in combination with the indicated concentration of AR6 for 30 minutes, AMD3100 was used as the positive control compound. **(A)** Phosphorylations of AKT and ERK induced by SDF-1 α were significantly inhibited by AR6. **(B)** The band density ratios (% control) were calculated using ImageJ and Prism GraphPad 7. **, p value < 0.005.

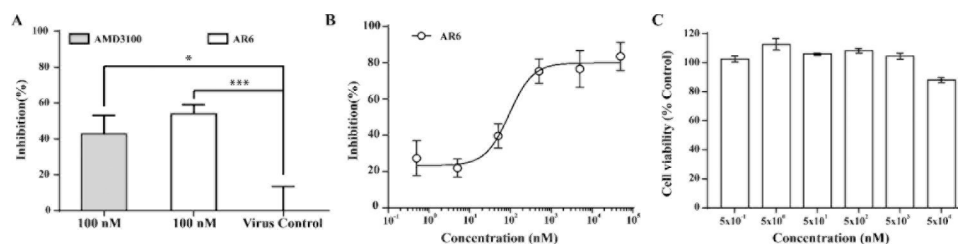


Figure 4.

Anti-HIV-1 activities and PBMC cytotoxicities of AR6. **A)** AR6 blocked HIV-1 entrance into PBMCs, and AR6 showed better activity than AMD3100 after exposed to the virus for 24 hours. The concentration of AR6 and AMD3100 was 100 nM. The inhibition values were calculated by GraphPad Prism 7 and the results are mean \pm SD of at least three independent experiments. *, p value < 0.05, ***, p value < 0.0005. **B)** The IC₅₀ value of AR6 was 93 nM after a 2-hour viral exposure followed by a five-day culture. The anti HIV-1 assay results were determined by quantifying the extracellular p24 antigens. **C)** AR6 at the concentrations used for blocking HIV-1 entry did not show detectable cytotoxicity using the CellTiter-Bule assay.

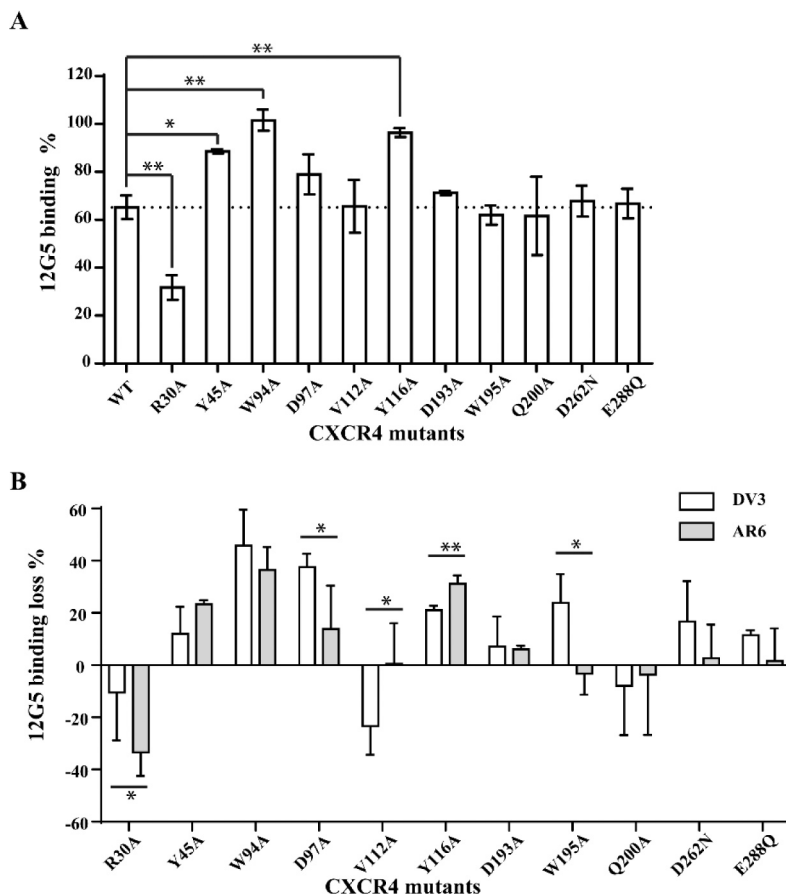


Figure 5. Binding activity of AR6 to WT CXCR4 and mutants. (A) The CXCR4 binding affinity of AR6 was decreased by mutations Y45A, W94A, Y116A whereas the binding affinity of AR6 was increased by mutation R30A. The other CXCR4 mutations had little effect on AR6 binding affinity. (B) Compared with the DV3 fragment, AR6 and DV3 can both interact with CXCR4 mutants Y45, W94 and Y116A. The data represent the mean values of three independent experiments with the error bars indicated as SD. *, p value < 0.05, **, p value < 0.005.

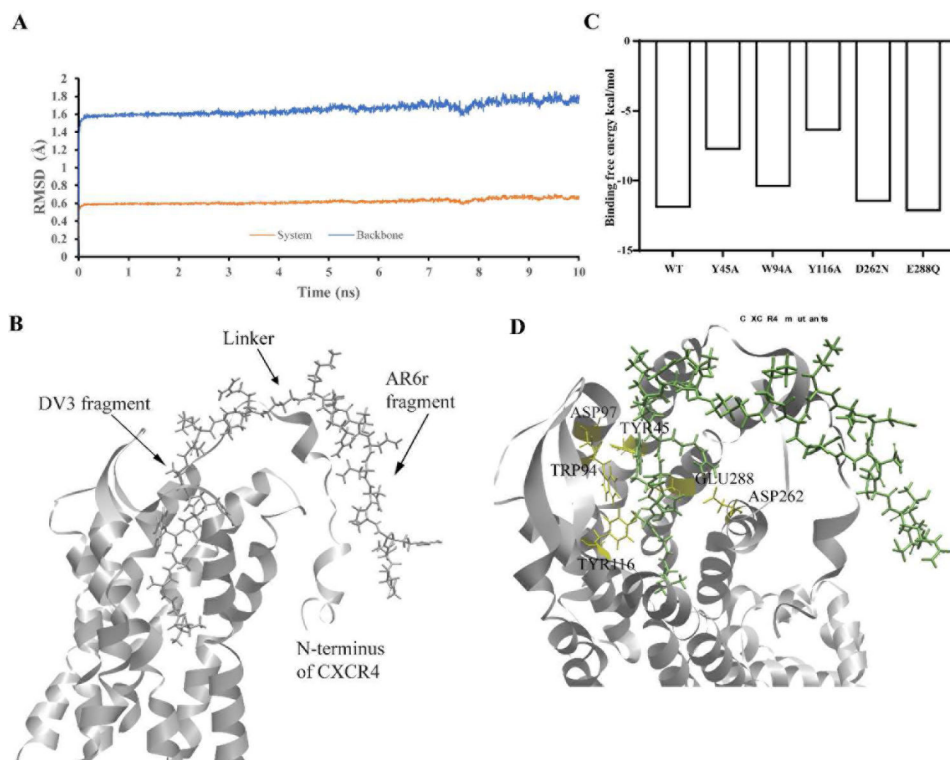
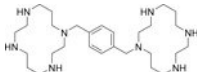


Figure 6. MD simulation and binding free energy calculations of CXCR4 interaction with AR6. **(A)** MD simulation (10 ns) was carried out for AR6 in complex with CXCR4. Both the backbone and system reached the stable status at about 100 ps. **(B)** CXCR4 are shown in the ribbon model whereas AR6 peptide in stick. According to the MD results, the DV3 fragment of AR6 interacts with the TM domain of CXCR4, whereas the other fragment of AR6 (i.e., AR6r derived from the HIV-1 gp120 V3 loop) interacts with the CXCR4 N-terminus. **(C)** Binding free energy calculations of CXCR4 mutants as compared with wild type (WT) CXCR4. **(D)** Positions of CXCR4 residues used in binding free energy calculations.

Table 1.Amino acid sequences or chemical structure and IC₅₀ values in CXCR4 binding assays.

Name	Peptide sequence ^a	IC ₅₀ (μM)	
		CHO-CXCR4	Sup-T1
AR5	H ₂ N-Igaswhrpdkkr-Ahx-KRKGDIRQAHC-CONH ₂	0.018	0.023
AR6	H ₂ N-Igaswhrpdkkr-Ahx-KRKTNNNPRTC-CONH ₂	0.016	0.014
AR5r	H ₂ N-Ahx-KRKGDIRQAHC-CONH ₂	>50	>50
AR6r	H ₂ N-Ahx-KRKTNNNPRTC-CONH ₂	9.12	7.418
DV3	H ₂ N-Igaswhrpdk-CONH ₂	1.10	0.615
DV3kr	H ₂ N-Igaswhrpdkkr-CONH ₂	0.474	ND ^b
AMD3100		0.051	0.044

^aLowercase letters denote D-amino acids.^bND = not determined

Table 2.

Binding free energy values of wild type (WT) CXCR4 and mutants.

CXCR4 mutants	ddG_elec ^a	ddG_nonelec ^b	dG_bind ^c
WT	-10.51	-1.37	-11.88
Y45A	-7.45	-0.28	-7.73
W94A	-7.87	-2.51	-10.38
D97A	-6.21	-5.26	-11.84
Y116A	-4.51	-1.83	-6.34
D262N	-8.90	-2.54	-11.44
E288Q	-10.67	-1.46	-12.13

^addG_elec represents electrostatic interaction contribution to the binding free energy.

^bddG_nonelec represents nonelectrostatic interaction contribution to the binding free energy.

^cdG_bind represents the total binding free energy.